Carbon Formation and CO Methanation on Silica-Supported Nickel and Nickel–Copper Catalysts in CO + H$_2$ Mixtures

M. T. Tavares,* I. Alstrup,† C. A. Bernardo,* and J. R. Rostrup-Nielsen†

*School of Engineering, Universidade do Minho, P-4800 Guimarães, Portugal; and †Haldor Topsøe Research Laboratories, Nymøllevej 55, DK-2800 Lyngby, Denmark

The steady-state rates of simultaneous carbon formation and methanation on silica-supported nickel and nickel–copper catalysts in CO + H$_2$ gas mixtures have been measured in the partial pressure range 10–30 kPa and the temperature range 583–873 K. The steady-state kinetic results for carbon formation can be explained by a model previously used for carbon formation in pure CO gas, but modified to take into account the influence of hydrogen. Comparisons between the results for Ni/SiO$_2$, Ni$_{0.99}$Cu$_{0.01}$/SiO$_2$, Ni$_{0.9}$Cu$_{0.1}$/SiO$_2$, and Ni$_{0.75}$Cu$_{0.25}$/SiO$_2$ show that the specific rate of carbon formation is increased when 1 at.% of Cu is added to a nickel catalyst, but that the rate decreases when the Cu content is increased to 10 at.%, and that no carbon formation is seen for the Ni$_{0.75}$Cu$_{0.25}$/SiO$_2$ catalyst. The addition of a small amount of Cu, on the other hand, decreases the methanation rate while at higher Cu contents the rate goes up again and a maximum is observed at about 7 at.% Cu. Thus a simple ensemble model cannot explain the influence of copper on the rate of carbon formation or methanation. Comparison of carbon formation and methanation rates for the Ni/SiO$_2$ and the Ni$_{0.99}$Cu$_{0.01}$/SiO$_2$ catalysts indicates that the two reactions have different rate-controlling steps and that the carbon formation influences the methanation rate mainly through poisoning of the catalysts. © 1996 Academic Press, Inc.

1. INTRODUCTION

Carbon formation on transition metal catalysts from the decomposition of hydrocarbons or carbon monoxide has been studied extensively for many years. One major reason for this interest in carbon formation is that it can cause very important operational problems in a number of industrial catalytic processes (1). Under usual conditions, long carbon filaments grow out of the catalytic metal particles without blocking the processes responsible for their growth. In this way accumulation of huge amounts of carbon in and on the catalyst pellets is possible, which can create very severe problems in the reactors.

One way to reduce the risk of carbon filament growth is to add to the surface an agent which poisons the carbon formation reaction more than the desired process. In industrial steam reforming this can be achieved by using sulfur as the selective poisoning agent (2). A similar effect might be obtained by adding copper to the nickel surface (3).

Recently, Alstrup and Tavares (4) showed that kinetic data for carbon formation on a Ni/SiO$_2$ catalyst from CH$_4$ + H$_2$ gas mixtures can be explained by a kinetic model similar to one suggested previously by Grabke (5) for carbon formation on iron but with another rate-controlling step, the dissociative chemisorption of CH$_4$. The same type of model could also explain the observed rates for a Ni$_{0.99}$Cu$_{0.01}$/SiO$_2$ catalyst, which were higher than for the Ni/SiO$_2$ catalyst. On the other hand, it could only explain the rates for a Ni$_{0.9}$Cu$_{0.1}$/SiO$_2$ catalyst at low carbon activities, where the rates were much lower than for the Ni/SiO$_2$ catalyst. At higher carbon activities the observed rates increased much faster than predicted by the model. Alstrup and Tavares (6) were also able to construct a microkinetic model based on experimental and theoretical values for the binding and vibrational energies of the surface species involved. However, the modeling indicated that the assumption of a single rate-controlling step is not realistic, but that both the chemisorption step and the first dehydrogenation step are far from equilibrium. Very recently Tavares *et al.* (7) reported studies on Ni/SiO$_2$ and NiCu/SiO$_2$ catalysts of the equilibrium of carbon formation in CO + CO$_2$ gas mixtures and of the kinetics of carbon formation in pure CO. It was found that the kinetics could be explained by a model based on disproportionation of CO as the rate-controlling step. The rate of carbon formation on the Ni$_{0.9}$Cu$_{0.1}$/SiO$_2$ was also lower than for the Ni/SiO$_2$ catalyst and the dependence on the CO pressure was weaker.

The influence of Cu in NiCu catalysts on various hydrocarbon reactions including CO methanation has previously been discussed in several papers (8–12). Ponec (8) and Sachtler and van Santen (9) have reviewed work up to 1983 and 1977, respectively. The dependence of the reactivity of the alloy catalysts on the composition of the metal particles has often been discussed from the point of view of ensem-

ble theory. Ensemble theories have in particular been discussed by Martin and Dalmon (10–13), by Andersen *et al.* (14), and by Alstrup and Andersen (14). Martin and Dalmon (11, 12) used a simple ensemble model for the interpretation of the copper dependence of the rates, i.e., they used the expression

$$\text{rate}(\theta_{Cu}) = k_0(1 - \theta_{Cu})^N, \qquad [1]$$

where k_0 is the rate for 0 at.% Cu, θ_{Cu} is the copper surface coverage of the alloy particles, and N is the number of atoms required for a surface ensemble of nickel atoms to be able to catalyze the process. For CO methanation they found $N = 13 \pm 2$. On the other hand, Bernardo *et al.* (3) found that rates of carbon formation from $CH_4 + H_2$ gas mixtures on NiCu alloy catalysts were not compatible with an ensemble theory.

In the present work we have studied the influence of hydrogen on the rate and the mechanism of carbon formation from CO on the same types of silica-supported nickel and nickel–copper catalysts as in our previous carbon formation studies (3, 4, 6, 7). In addition we have measured the rate of CO methanation taking place simultaneously with the carbon formation. The rates of carbon formation are discussed on the basis of the model developed to explain the rates of carbon formation by disproportionation of CO (7). Also the dependences of the rates of carbon formation and methanation on the copper content of the catalyst and the relation between carbon formation and methanation are discussed.

2. EXPERIMENTAL

2.1. Preparation of Catalysts

The Ni/SiO₂ and NiCu/SiO₂ catalysts were prepared by "dry" impregnation with 20 wt.% metal phase Cu:(Ni + Cu) ratios of 0, 0.01, 0.1, and 0.25. The required amounts of nickel and copper nitrates were dissolved in an amount of water equal to the measured pore volume (1.89 ml/g) of the silica powder (Cab-O-Sil H₅ from Cabot Corp., BET area: 325 m²/g) used as support material. The solution and the support material were mixed, dried at room temperature, and calcined at 773 K for 3 h. The resulting powder was mixed in a mortar with 1% methyl-cellulose-ether plasticizer (Methocel A4C from Dow Chemical Co.) and water. The final paste was extruded in small, cylindrical pellets with 4 mm diameter and 4 mm length. The pellets were calcined for 2 h at 873 K and prereduced at 773 K in H₂ for 44 h.

2.2. Characterization of Catalysts

The samples were characterized by hydrogen chemisorption, nitrogen adsorption, X-ray diffraction and by trans-

mission and scanning electron microscopy. The composition of the catalysts was checked by elemental chemical analysis.

2.3. Reactor System and Reactants

The determination of the rate of carbon formation was based on monitoring the weight variations of the catalyst samples under reaction conditions by means of a C.I. Electronics MK IIB microbalance. The microbalance has a capacity of 1 g and a sensitivity of 1 μg. The sample was suspended in a silica basket inside a flow reactor with associated furnace and flow and temperature controllers. A thermocouple was placed inside the reactor, close to the sample, in the flat part of the furnace temperature profile. The temperature of the reactor wall was measured by another thermocouple at the same level as the sample.

The methanation rate was measured on-line by means of a Pye Unicam gas–solid chromatograph. A small part of the exit gas went through a six-port valve (Pye Unicam 104). A column with Poropak Q 80/100 mesh heated to 373 K was used together with a hydrogen–air flame ionization detector for the measurements of the methane concentration.

The gases used (CO, H₂, and N₂) were of high purity (>99.95%). The hydrogen was cleaned further by being passed through a Cu furnace, held at 523 K, and mixed with the other reactants in a silica gel and in a 4A molecular sieve trap.

2.4. Experimental Conditions

The system was cleaned by an N₂ flow before each run. All samples were reduced for 1 h in a hydrogen flow of 6.7×10^{-5} mol s⁻¹ after which the temperature of the sample was adjusted to the selected reaction temperature and the system was cleaned again by a flow of N₂. A total flow of 2.98×10^{-4} mol s⁻¹ of reactants was admitted to the reactor when the temperature had stabilized. The balance was made with nitrogen. The rates of carbon deposition were determined from the slopes of the straight line parts of the curves drawn by the microbalance recorder after the initial transients had died out subsequent to a change of conditions. The same steady-state rate of weight change was observed whether the changes were from higher or from lower values of the partial pressure of CO or H₂. A fresh sample was used in each isothermal run.

A few experiments were made to investigate whether the temperature measured outside the sample was different from the sample temperature. In those experiments a Ni/SiO₂ catalyst was suspended, attached to a thermocouple in the center of the catalyst sample. The tests were made at typical conversions attained in this work, 0.3–0.6%, and at temperatures between 650 and 715 K. The difference between the temperatures measured by the two thermo-

TABLE 1

Hydrogen Chemisorption Results

Catalyst	Total H_2 (μmol/g)	Strongly bound H_2 (μmol/g)
Ni/SiO_2	166	88
$Ni_{0.99}Cu_{0.01}/SiO_2$	64	36
$Ni_{0.9}Cu_{0.1}/SiO_2$	37	10
$Ni_{0.75}Cu_{0.25}/SiO_2$	31	4

couples was in all cases in the range 1–3 K, i.e., within the uncertainty of the measurements.

3. RESULTS

3.1. Catalysts

The fresh Ni/SiO_2 and $NiCu/SiO_2$ catalysts had a BET area of 250 m^2 g^{-1}, which after carbon deposition was reduced to about 150 m^2 g^{-1}. The average pore radius changed from 6.7 nm for the fresh catalysts to ca. 9 nm after deposition. The width of the X-ray diffraction peaks indicated an average diameter of the metal crystallites of about 24 nm, with a slightly lower value for the $Ni_{0.99}Cu_{0.01}/SiO_2$ catalyst than for the other ones. The total hydrogen uptake and the chemisorption of "strongly held" hydrogen (3) was determined for the fresh catalysts at 298 K and at hydrogen pressures in the range 5–15 kPa. The results are shown in Table 1. The results obtained for the $Ni_{0.9}Cu_{0.1}/SiO_2$ and $Ni_{0.75}Cu_{0.25}/SiO_2$ catalysts relative to the results for Ni/SiO_2 catalyst are very similar to the results obtained in Ref. (3). For the $Ni_{0.99}Cu_{0.01}/SiO_2$ catalyst the relative values are lower than in Ref. (3). In Ref. (3) it was con-

cluded on the basis of the significant drop in strongly held hydrogen with increased Cu concentration that copper surface segregation had taken place on the alloy particles. This conclusion was also supported by XPS measurements. The same conclusion may be made for the fresh alloy catalysts of the present study. It should be stressed, however, that the composition of the alloy surfaces during steady-state reaction is not known.
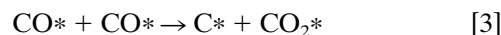
3.2. Experimental Carbon Formation and Methanation Rates

Experiments were made for a number of temperatures in the range 573–873 K. The CO and H_2 partial pressures were varied independently. The CO pressures used were 10, 20, and 30 kPa and the H_2 pressures were 10, 15, 20, 25, and 30 kPa. A selection of the most interesting rate results obtained are shown in Tables 2–4. Under conditions where the rates were below the limit of detection no rate values are given in the tables.

4. DISCUSSION

4.1. Carbon Formation

Recently Tavares *et al.* (7) used a kinetic model based on the elementary steps

$$CO + * \rightleftarrows CO* \qquad [2]$$

$$CO* + CO* \rightarrow C* + CO_2* \qquad [3]$$

$$CO_2* \rightarrow CO_2 + * \qquad [4]$$

to explain the observed kinetics of carbon formation from CO on the same type of Ni/SiO_2 and $NiCu/SiO_2$ catalysts as used in the present work. With the assumptions that

TABLE 2

Rates of Carbon Formation and Methanation at Various Temperatures on Ni/SiO_2

P_{CO} (kPa)	P_{H_2} (kPa)	Rates of C formation (r_C, in units of mg s^{-1} mg^{-1}) and methanation (r_{CH_4}, in units of ml s^{-1} mg^{-1})							
		623 K		673 K		723 K		773 K	
		$r_C \times 10^6$	$r_{CH_4} \times 10^3$	$r_C \times 10^6$	$r_{CH_4} \times 10^3$	$r_C \times 10^6$	$r_{CH_4} \times 10^3$	$r_C \times 10^6$	$r_{CH_4} \times 10^3$
20	10	5.36			2.66	19.3	3.06	23.8	2.15
	15	2.95	2.52		2.80	0.58	3.33	14.4	2.31
	20	2.21	2.64		2.92		4.29	5.07	2.80
	25		2.79		3.23		4.54	3.76	2.86
	30		2.97		3.45		5.64	1.57	3.41
30	10	3.93		33.5	2.63	23.0	2.71	338.0	2.58
	15		2.40	22.4	3.04	21.3	3.79	26.4	2.86
	20		2.55	12.0	3.13	11.5	3.95	6.59	3.24
	25		2.66	10.2	3.31	2.94	4.01	2.50	3.49
	30		2.69	7.18	3.59	0.58	5.03	0.73	4.45

TABLE 3

Rates of Carbon Formation and Methanation at Various Temperatures on $Ni_{0.99}Cu_{0.01}/SiO_2$

P_{CO} (kPa)	P_{H_2} (kPa)	Rates of C formation (r_C, in units of mg s^{-1} mg^{-1}) and methanation (r_{CH_4}, in units of ml s^{-1} mg^{-1})							
		673 K		723 K		773 K		873 K	
		$r_C \times 10^6$	$r_{CH_4} \times 10^3$	$r_C \times 10^6$	$r_{CH_4} \times 10^3$	$r_C \times 10^6$	$r_{CH_4} \times 10^3$	$r_C \times 10^6$	$r_{CH_4} \times 10^3$
10	10	0.32	0.73	0.61	2.27	1.05		7.96	
	15	0.21	0.98	0.22	2.51		1.10	2.66	1.94
	20	0.17	1.30	0.20	2.74		1.32	0.55	2.17
	25		1.63		2.92		1.43	0.38	2.31
	30		1.96		3.25		1.54	0.29	2.35
20	10	2.02	2.23	11.3	1.92	27.8	0.53	23.9	
	15	0.29	2.62	2.68	2.70	17.5	0.84	13.7	2.23
	20	0.27	2.86	0.39	3.17	0.21	1.26	7.98	2.53
	25		3.05	0.14	3.88		1.68	7.31	2.92
	30		3.44		4.58		2.00	5.54	2.92
30	10	3.64	2.35	50.0	1.84	41.4	2.26	59.4	2.10
	15	1.49	3.25	34.3	3.21	33.2	2.60	41.2	2.69
	20	0.42	3.55	22.9	3.49	24.7	3.33	21.7	3.29
	25		3.65	15.4	4.58	22.4	3.50	15.4	3.70
	30		4.15	10.3	5.56	16.1	4.07	7.41	4.03

step [3] is rate-controlling, that step [2] is in quasi-equilibrium, that step [4] is irreversible due to the absence of CO_2 in the feed, and that the adsorbed species are competing for the same type of sites on the surface, a rate expression is easily derived (7),

$$r_3 = k_3 \frac{K_2^2 P_{CO}^2}{(1 + K_2 P_{CO})^2},\qquad [5]$$

where k_3 is the rate constant of step [3] and K_2 is the equilibrium constant of step [2]. The simplest way of taking the presence of hydrogen atoms on the surface into account in this model would be to add a hydrogen chemisorption step,

$$H_2 + 2* \rightleftarrows 2H*,\qquad [6]$$

assuming that step [6] is in quasi-equilibrium and that hydrogen atoms are competing with the CO molecules for the same surface sites. The rate expression for carbon formation then becomes

$$r_3 = k_3 \frac{K_2^2 P_{CO}^2}{(1 + K_2 P_{CO} + K_6^{1/2} P_{H_2}^{1/2})^2},\qquad [7]$$

where K_6 is the equilibrium constant of step [6].

However, it turns out that the hydrogen dependence of expression [7] is much too weak to describe the observed

TABLE 4

Rates of Carbon Formation and Methanation at Various Temperatures on $Ni_{0.9}Cu_{0.1}/SiO_2$

P_{CO} (kPa)	P_{H_2} (kPa)	Rates of C formation (r_C, in units of mg s^{-1} mg^{-1}) and methanation (r_{CH_4}, in units of ml s^{-1} mg^{-1})							
		623 K		673 K		723 K		773 K	
		$r_C \times 10^6$	$r_{CH_4} \times 10^3$	$r_C \times 10^6$	$r_{CH_4} \times 10^3$	$r_C \times 10^6$	$r_{CH_4} \times 10^3$	$r_C \times 10^6$	$r_{CH_4} \times 10^3$
20	30		2.53		4.77		7.32		4.39
30	10				2.97	0.69	3.77	1.83	2.80
	15				3.29	0.39	5.45	1.25	3.59
	20				3.55	0.15	5.63	0.92	4.10
	25				4.63		6.10	0.52	4.54
	30		2.18		4.73		6.34	0.39	5.16

<div style="text-align: center">

TABLE 5

**Parameters of Kinetic Model for Carbon Formation on
NiCu/SiO$_2$ in CO + H$_2$**

</div>

Cu (at.%)	T (K)	E_{H^*} (kJ/mol)	$E_{CO^*}(0)$ (kJ/mol)	α (kJ/mol/ML)
0	723	250	120	50
0	773	250	120	90–100
1	673	245	110	71
1	723	245	110	50
1	773	245	110	38
1	873	245	110	94
10	723	242	105	92
10	773	242	105	77

FIG. 1. Rates of carbon formation on Ni/SiO$_2$ as function of hydrogen pressure. $T = 723$ K, $P_{CO} = 30$ kPa (■) and 20 kPa (△). Curves are calculated using expressions [7] and [8].

hydrogen dependence of the carbon formation rates. This failure is in accordance with the observation in several papers (16–19) that coadsorbed hydrogen has a strong influence on the adsorption of CO. The adsorbed hydrogen and CO can be either segregated or mixed. The mixed phases are formed on the open surfaces Ni(100) and Ni(110), and here the presence of hydrogen lowers the chemisorption energy of CO locally (16–19). The hydrogen coverage dependence of the CO chemisorption bond energy, E_{CO^*}, cannot be determined from the published coadsorption studies. Consequently, to investigate whether the influence of coadsorbed hydrogen can qualitatively explain the observed hydrogen dependence of the carbon formation rate we use the simple assumption of a linear dependence on the hydrogen coverage, θ_H,

$$E_{CO^*}(\theta_H) = E_{CO^*}(0) - \alpha\theta_H. \quad [8]$$

The rates of carbon formation as function of hydrogen pressure have been calculated using expression [7]. The equilibrium constants, K_2 and K_6, are assessed by first calculating the partition functions of the adsorbed and the gaseous species as discussed in Refs. (6) and (20). The vibrational and rotational data used for hydrogen are shown in Ref. (6) and for carbon monoxide in Ref. (7). The binding energy used for chemisorbed carbon monoxide, $E_{CO^*}(\theta_H)$, is calculated using expression [8], with α treated as an adjustable parameter. The values used for $E_{CO^*}(0)$ and for the binding energy of chemisorbed hydrogen atoms, E_{H^*}, are shown in Table 5 together with the values of α. Some of the results obtained are shown in Figs. 1–5. The binding energy used for chemisorbed hydrogen atoms is close to the one used in the successful modeling of carbon formation from CH$_4$ + H$_2$ mixtures in Ref. (6). It is slightly lower than the experimental values for clean nickel single-crystal surfaces. Many measurements of the binding energy of CO on nickel surfaces have been reported in the literature. The most recent determination is the microcalori-
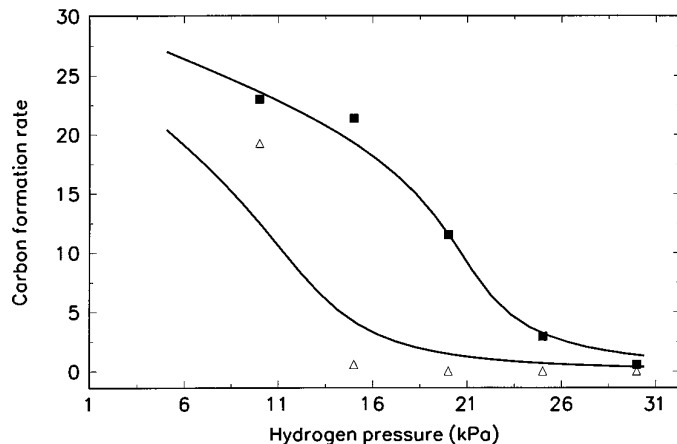
metric study by Stuckless *et al.* (21). In the present modeling, as in the previous studies (4, 6, 20), data for the Ni(100) surface have been used. The CO binding energy varies from 123 kJ/mol for the clean surface to 99 kJ/mol for a CO coverage of about 0.8 ML (21). The value used here, 120 kJ/mol, is a reasonable compromise in the temperature range considered where the coverage is quite low. We choose not to distinguish between linear and bridge-bonded CO because it has recently been shown by Grossman *et al.* (22) and by Yoshinobu *et al.* (23) that the difference in chemisorption bond energy between the two types is negligible on Ni(100) (of the order of 1–2 kJ/mol). Thus in the case of the nickel catalyst only two parameters, the rate constant k_3 and α, are adjusted for each temperature. The shapes of the curves are determined solely by α be-
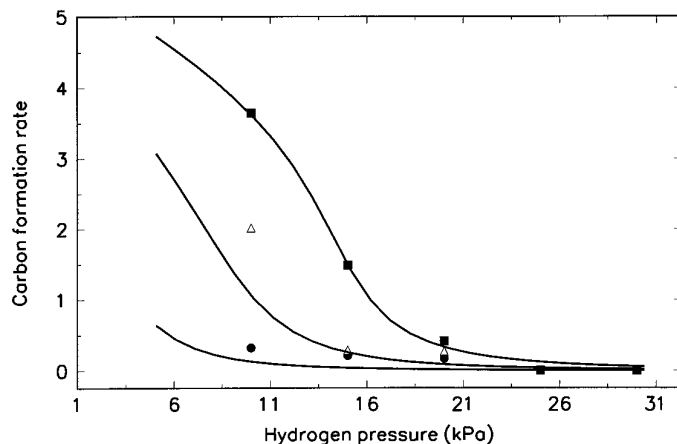

FIG. 2. Rates of carbon formation on Ni$_{0.99}$Cu$_{0.01}$/SiO$_2$ as function of hydrogen pressure. $T = 673$ K, $P_{CO} = 30$ kPa (■) and 20 kPa (△), and 10 kPa (●). Curves are calculated using expressions [7] and [8].
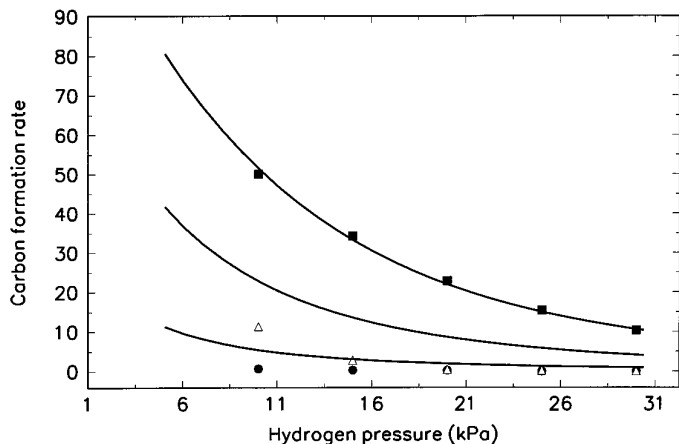
FIG. 3. Rates of carbon formation on $Ni_{0.99}Cu_{0.01}/SiO_2$ as function of hydrogen pressure. $T = 723$ K, $P_{CO} = 30$ kPa (■), 20 kPa (△), and 10 kPa (●). Curves are calculated using expressions [7] and [8].
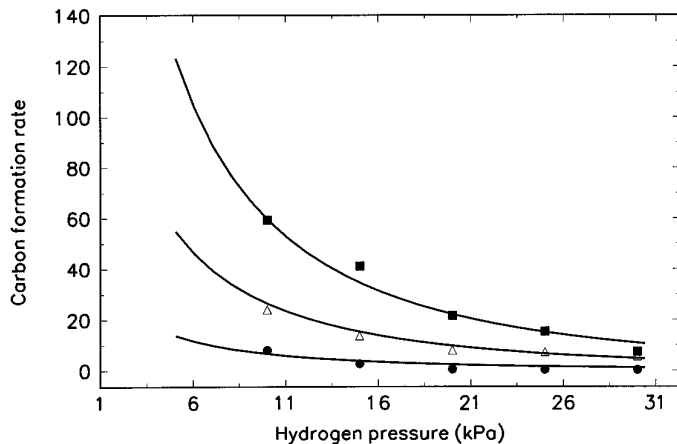

FIG. 5. Rates of carbon formation on $Ni_{0.99}Cu_{0.01}/SiO_2$ as function of hydrogen pressure. $T = 873$ K, $P_{CO} = 30$ kPa (■), 20 kPa (△), and 10 kPa (●). Curves are calculated using expressions [7] and [8].

cause k_3 acts only as a scaling parameter. It was found that, when the catalysts contain copper, a small reduction of the binding energies, as shown in Table 5, improves the agreement between model and experiment. The good overall agreement, in particular at $P_{CO} = 30$ kPa, between calculated and measured (nonnegligible) rates indicates that the model contains the most important elements of the mechanism of carbon formation on nickel and nickel–copper catalysts in $CO + H_2$ mixtures.

The carbon formation rates for the $NiCu/SiO_2$ catalysts relative to the rates for the Ni/SiO_2 catalyst are shown in Fig. 6 as functions of the hydrogen partial pressure. It is seen that at the higher hydrogen pressures the carbon formation is strongly promoted by the addition of 1 at.% Cu but is poisoned by higher amounts of copper under all conditions.
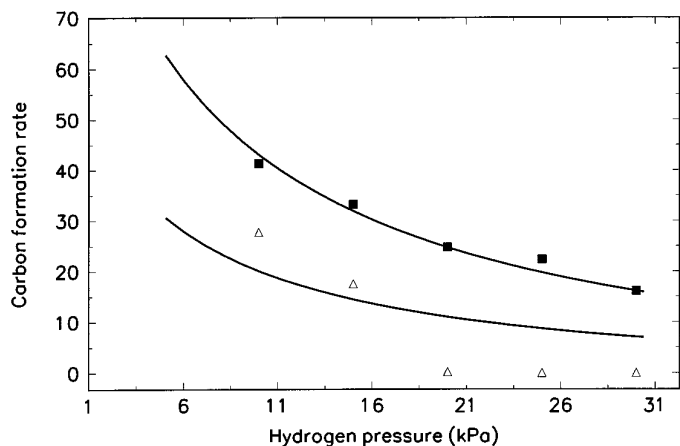
4.2. Relation between Carbon Formation and Methanation

The carbon formation rates are plotted versus methanation rates in Fig. 7 for the Ni/SiO_2 catalyst and in Fig. 8 for the $Ni_{0.99}Cu_{0.01}/SiO_2$ catalyst. In spite of the scatter in the plots, a clear tendency is seen, most pronounced at the highest CO pressure, 30 kPa (filled symbols), toward an inverse relationship between the two rates, i.e., a large carbon formation rate corresponds to a low methanation rate and vice versa, indicating that the two reactions have different rate-controlling steps. This is in agreement with the kinetic model for carbon formation discussed above, where the disproportionation of adsorbed CO is rate-controlling, and with the kinetic model for the methanation reaction on nickel suggested by Alstrup (20), according to
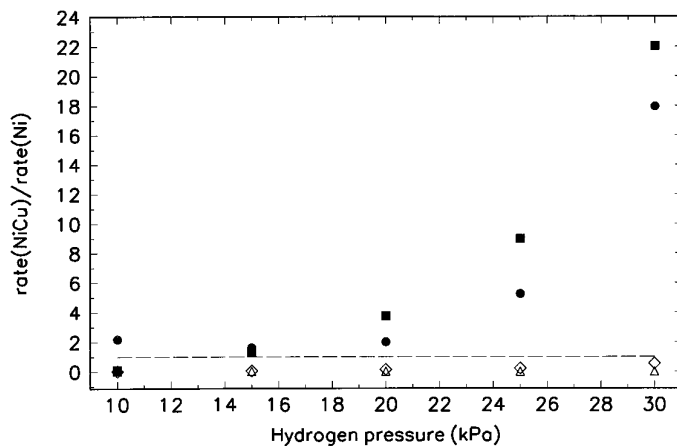

FIG. 4. Rates of carbon formation on $Ni_{0.99}Cu_{0.01}/SiO_2$ as function of hydrogen pressure. $T = 773$ K, $P_{CO} = 30$ kPa (■) and 20 kPa (△). Curves are calculated using expressions [7] and [8].

FIG. 6. Rates of carbon formation on $Ni_{0.99}Cu_{0.01}/SiO_2$ at $T = 723$ K (●) and 773 K (■), and on $Ni_{0.9}Cu_{0.1}/SiO_2$ at $T = 723$ K (△) and 773 K (◇), as function of hydrogen pressure. $P_{CO} = 30$ kPa.
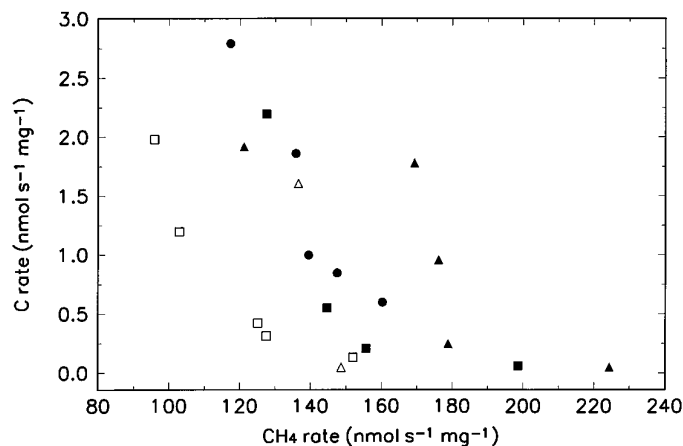
FIG. 7. Rates of carbon formation on Ni/SiO$_2$ versus rates of simultaneous methanation. $T = 673$ K (●), 723 K (△, ▲), and 773 K (□, ■). Open symbols, $P_{CO} = 20$ kPa; filled symbols, $P_{CO} = 30$ kPa.

which hydrogenation of CH* surface species is rate-controlling.

Although it is expected that the main part of the carbon formed on Ni and NiCu catalysts under the present conditions grows out of the metal particles as long filaments, which do not poison the surface on which the catalytic reaction takes place (24), it is conceivable that a small part of the carbon atoms on the surface form C–C bonds to other C atoms on the surface. In this way, patches of graphite are poisoning part of the surface at a rate proportional to the overall carbon formation rate, explaining the trends seen in Figs. 7 and 8.

4.3. Cu Concentration Dependence of the Activities

In several previous studies of catalytic reactions on NiCu catalysts ensemble models have been used in the discussion
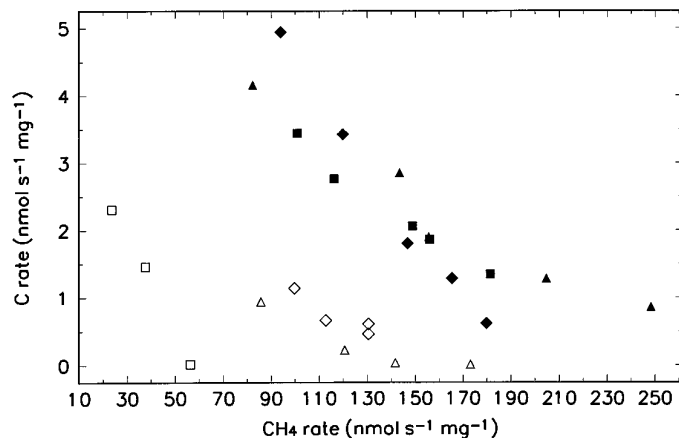

FIG. 8. Rates of carbon formation on Ni$_{0.99}$Cu$_{0.01}$/SiO$_2$ versus rates of simultaneous methanation. $T = 723$ K (△, ▲), 773 K (□, ■), and 873 K (◇, ◆). Open symbols, $P_{CO} = 20$ kPa; filled symbols, $P_{CO} = 30$ kPa.

of composition dependences (8–13). By applying expression [1] to measurements of the rates of CO methanation on NiCu/SiO$_2$ catalysts, Dalmon and Martin (11) concluded that ensembles of ca. 13 Ni atoms are required for this process to take place. Ensemble models can of course be applied only if the surface concentration and distribution of copper and nickel atoms during reaction are known. Dalmon and Martin (11) concluded from hydrogen chemisorption and magnetic studies that the surface composition of the metallic particles of their catalysts was very similar to the bulk composition. Martin (13) discussed previous investigations of the short-range order in the distribution of nickel and copper atoms in the surface of NiCu alloys and concluded that the distribution is not random for a sample which has been cooled slowly from a high annealing temperature, while no short-range order will be present if the sample has been rapidly quenched. No information is available about the distribution during reaction. Bernardo et al. (3) showed by hydrogen chemisorption and XPS measurements that the surface of the alloy particles of the reduced NiCu/SiO$_2$ catalysts, prepared in the same way as the ones used in the present work, were enriched in copper compared to the bulk composition, in agreement with the copper surface enrichment generally observed on macroscopic samples of NiCu alloys. Bernardo et al. (3) suggested that the lack of copper enrichment of the samples of Dalmon and Martin might be due to the high reduction temperature (920 K) used by them, which makes possible prevention of surface segregation because of incorporation in the surface of Si atoms from the support.

A precondition for attributing a critical ensemble size to a reaction is that a straight line is obtained in a logarithmic plot of rate versus Ni surface concentration in accordance with expression [1]. Bernardo et al. (3) found, as mentioned above, that this condition was not fullfilled for their carbon formation results. Nor are the present results in agreement with this condition. As already mentioned, the carbon formation at the higher hydrogen pressures is strongly promoted by increasing the Cu concentration from 0 to 1 at.%, but decreases strongly when the Cu concentration is increased to 10 at.%.

The methanation rates in Tables 2–4 also depend nonmonotonically on the Cu concentration. At $P_{CO} = 20$ kPa, $P_{H_2} = 30$ kPa, and $T = 723$ K the rate is decreased by about 20% when the Cu content is increased from 0 to 1 at.%, but it is increased by about 30% when going from 0 to 10 at.% Cu and decreased by about 70% in going from 0 to 25 at.% Cu. To investigate this dependence closer, a new series of NiCu/SiO$_2$ catalysts with Cu concentrations 0, 1, 2, 5, 7, 10, 15, and 20 at.% was prepared as before and methanation rates were measured at the above conditions, i.e., at $P_{CO} = 20$ kPa, $P_{H_2} = 30$ kPa, and $T = 723$ K. The results obtained are shown in a logarithmic plot in Fig. 9 (open symbols) together with the above mentioned
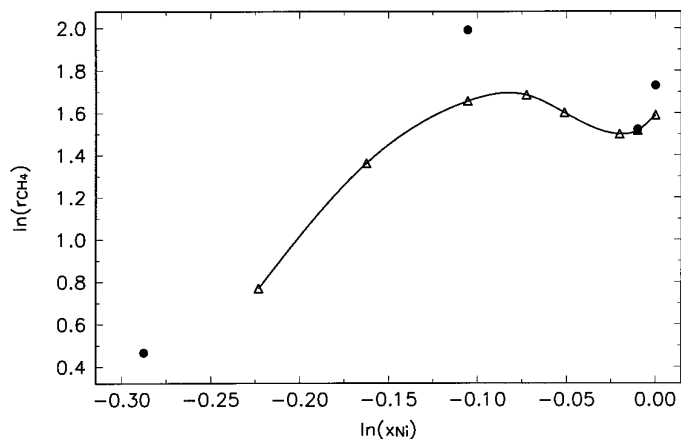
FIG. 9. Logarithmic plot of rates of methanation on Ni_xCu_{1-x}/SiO_2 catalysts as a function of x. $P_{CO} = 20$ kPa, $P_{H_2} = 30$ kPa, $T = 723$ K. Filled symbols, results from Tables 2–4.

results from Tables 2–4 (filled symbols). It is seen that the rates of this series show qualitatively the same behavior as a function of the Cu concentration with a maximum at about 7 at.% Cu, but with a smaller variation than the results from Tables 2–4.

The inverse relation between carbon formation and methanation rate shown in Figs. 7 and 8 may help to explain that the addition of 1 at.% Cu promotes carbon formation and has the opposite influence on the methanation reaction. It is to be expected that the surface concentration of carbon atoms increases when a small amount of Cu is added to nickel, reducing the rate of hydrogenation to methane. This means that the carbon filament growth increases and that, at the same time, the increased surface poisoning reduces the methanation rate further. However, higher Cu concentrations strongly diminish the carbon poisoning of the methanation reaction due to the strong reduction of the carbon formation rate.

The hydrogen and carbon monoxide binding energies used in modeling the kinetics of carbon formation on the NiCu catalysts were, as mentioned above, sligthly lower than the values used for the nickel catalyst. Comparison between model and experiment does not allow a very accurate determination of these changes in binding energies. However, it is in good agreement with experimental observations (25–27) to assume such a reduction. From the kinetic model of carbon formation [7] and the kinetic model of methanation on nickel, suggested by Alstrup (20) and tested on single-crystal and foil data, it can be concluded that the reduction of E_{CO*} does not influence directly the rate of carbon formation but promotes the rate of methanation. It is seen that the nominator and the denominator of the rate expression [7] depend in the same way on E_{CO*}. On the other hand, the main role of chemisorbed CO in methanation is to block active sites (20), with the conse-

quence that the overall activation energy of methanation is mainly determined by E_{CO*} at the lower temperatures. We may therefore suggest that the different dependences of carbon formation and methanation on the CO chemisorption energy explain why the latter is promoted and that the methanation rate has a maximum at a copper concentration which poisons the carbon formation.

5. CONCLUSIONS

The hydrogen pressure dependence of carbon formation rates on Ni/SiO_2 and $NiCu/SiO_2$ catalysts in $CO + H_2$ gas mixtures with partial pressures in the range 10–30 kPa and temperatures in the range 583–873 K can be qualitatively explained by the kinetic model derived for the carbon formation rates in pure CO, if it is taken into account that hydrogen coadsorbed with CO on nickel strongly weakens the chemisorption bond energy of CO.

Similar to what has been found previously in studies of carbon formation from $CH_4 + H_2$ and from CO on NiCu/SiO_2 catalysts, the present results show that a small concentration of Cu promotes the rate of carbon formation in $CO + H_2$ mixtures while higher Cu concentrations poison this reaction.

The rate of methanation on the $NiCu/SiO_2$ catalysts depends in a nonmonotonic way on the Cu concentration. A relative minimum is seen at about 2 at.% Cu and a maximum at about 7 at.% Cu and the rate decreases rapidly at higher Cu concentrations.

The Cu concentration dependence of the two reactions cannot be explained by a simple ensemble model.

REFERENCES

1. Rostrup-Nielsen, J. R., in "Catalysis, Science and Technology" (J. R. Anderson and M. Boudart, Eds.), Vol. 5, Chap. 1. Springer-Verlag, Berlin, 1984.
2. Rostrup-Nielsen, J. R., *J. Catal.* **85,** 31 (1984).
3. Bernardo, C. A., Alstrup, I., Rostrup-Nielsen, J. R., *J. Catal.* **96,** 517 (1985).
4. Alstrup, I., and Tavares, M. T., *J. Catal.* **139,** 513 (1993).
5. Grabke, H. J., *Metall. Trans.* **1,** 2972 (1970).
6. Alstrup, I., and Tavares, M. T., *J. Catal.* **135,** 147 (1992).
7. Tavares, M. T., Alstrup, I., Bernardo, C. A., and Rostrup-Nielsen, J. R., *J. Catal.* **147,** 525 (1994).
8. Ponec, V., *Adv. Catal.* **32,** 149 (1983).
9. Sachtler, W. M. H., and van Santen, R. A., *Adv. Catal.* **26,** 69 (1977).
10. Dalmon, J. A., and Martin, G. A., *J. Catal.* **66,** 214 (1980).
11. Dalmon, J. A., and Martin, G. A., in "Proceedings, 7th International Congress on Catalysis, Tokyo, 1980" (T. Seiyama and K. Tanabe, Eds.), p. 402. Elsevier, Amsterdam, 1981.

12. Martin, G. A., and Dalmon, J. A., *J. Catal.* **75,** 233 (1982).
13. Martin, G. A., *Catal. Rev. Sci. Eng.* **30,** 519 (1988).
14. Andersen, N. T., Topsøe, F., Alstrup, I., and Rostrup-Nielsen, J. R., *J. Catal.* **104,** 454 (1987).
15. Alstrup, I., and Andersen, N. T., *J. Catal.* **104,** 466 (1987).
16. Love, J. G., Haq, S., and King, D. A., *J. Chem. Phys.* **97,** 8789 (1992).
17. Haq, S., Love, J. G., and King, D. A., *Surf. Sci.* **275,** 170 (1992).
18. Tillborg, H., Nilsson, A., and Mårtensson, N., *Surf. Sci.* **273,** 47 (1992).
19. Rangelov, G., Bischler, U., Memmel, N., Bertel, E., Dose, V., Pabst, M., and Rösch, N., *Surf. Sci.* **273,** 61 (1992).
20. Alstrup, I., *J. Catal.* **151,** 216 (1995).
21. Stuckless, J. T., Al-Sarraf, N., Wartnaby, C., and King, D. A., *J. Chem. Phys.* **99,** 2202 (1993).
22. Grossman, A., Erley, W., and Ibach, H., *Phys. Rev. Lett.* **71,** 2078 (1993).
23. Yoshinobu, J., Takagi, N., and Kawai, M., *Phys. Rev. B* **49,** 16670 (1994).
24. Alstrup, I., *J. Catal.* **109,** 241 (1988).
25. Yu, K. Y., Ling, D. T., and Spicer, W. E., *J. Catal.* **44,** 373 (1976).
26. Prinsloo, J. J., and Gravelle, P. C., *J. Chem. Soc. Faraday Trans. 1* **76,** 2221 (1980).
27. Prinsloo, J. J., and Gravelle, P. C., *J. Chem. Soc. Faraday Trans. 1* **78,** 273 (1982).